The 2010 IEEE/RSJ International Conference on
Intelligent Robots and Systems
October 18-22, 2010, Taipei, Taiwan

Design and Compatibility of a High-Performance Actuation System for fMRI-Based Neuroscience Studies

M. Hara, *Member, IEEE,* J. Duenas, *Student Member, IEEE,* T. Kober, D. Chapuis, *Member, IEEE,* O. Lambercy, *Member, IEEE,* H. Bleuler, *Member, IEEE,* and R. Gassert, *Member, IEEE*

***Abstract*— Haptic interfaces compatible with functional magnetic resonance imaging (fMRI) are finding increasing interest as a tool to explore the neural correlates of human motor control and related dysfunctions. To achieve safety and MR compatibility, such devices have mainly relied on unconventional actuation methods suffering from limited bandwidth and non-linearities. This has resulted in complex control and restricted their use in applications involving fine and dynamic interaction with the hand and fingers. To address these limitations, we propose a concept for a shielded high-performance actuation system to be located inside the MR room, evaluate the effectiveness of the shielding and perform detailed MR compatibility tests. A conventional electromagnetic actuator is located within a steel shield to prevent mutual disturbance with magnetic fields of the scanner, which, together with power and control hardware, is placed within a Faraday cage with only a fiber-optical USB link to the control room. Detailed compatibility tests show that disturbing dynamic electromagnetic fields generated by the actuation system are well below the detectable threshold of the scanner, and actuator performance is not degraded by the MR environment. In combination with a light and stiff cable or rod transmission, the presented actuator technology, providing high transparency and force bandwidth, paves the way for fMRI-based neuroscience studies, e.g., to investigate the fine motor control of hand and fingers.**

I. Introduction

Functional magnetic resonance imaging (fMRI) is a well-established neuroimaging technique to infer human brain activity during cognitive and sensorimotor tasks. While electroencephalography (EEG) or magnetoencephalography (MEG) measure electrical brain signals from the cortex at several points over the skull with high temporal resolution, fMRI gives localized access to the entire brain by measuring hemodynamics related to brain activation with good spatial and temporal resolution. Over the past years, fMRI has found growing interest not only in clinical use, but also in neuroscience [1]–[3] and neurorehabilitation [4]. Together with the development of novel imaging techniques, compatible robotics technology has evolved, providing powerful tools to investigate the neural correlates of human motor control and related dysfunctions, such as impaired motor function following a cerebrovascular accident, in well-controlled and repeatable sensorimotor tasks. However, as MR systems employ a strong and homogeneous static magnetic field with an associated spatial gradient away from the imaging region, switching gradient fields, and powerful radio frequency (RF) pulses for imaging, they impose severe safety and compatibility constraints on robotic technologies to be used in such an environment [5], [6]. Robotic systems should not pose any safety hazard nor disturb the MR imaging, and, at the same time, should not be affected by the electromagnetic fields of the scanner. This limitation precludes the use of conventional electromagnetic actuators from applications in MR environments per se, and motivates the development of alternative actuation methods.

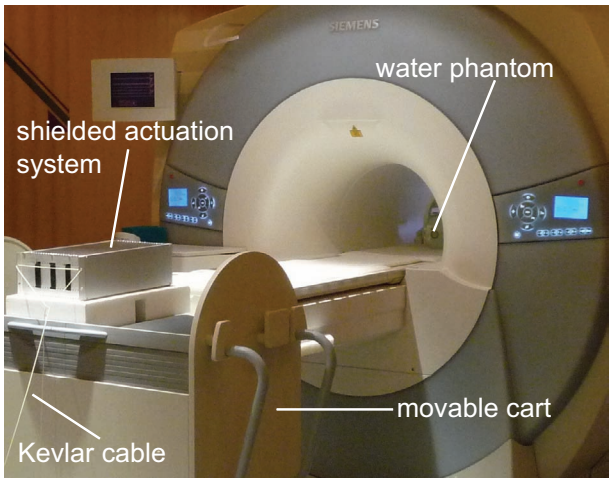

Fig. 1. Shielded actuation system placed at the end of the bed of a Siemens Tim Trio 3 T scanner for compatibility tests with a water phantom.

As candidates for MR-compatible actuation, piezoelectric actuators [7], hydraulic/pneumatic actuators and transmissions [8], [9], ultrasonic motors [10], [11], and electrostatic actuators [12] can be cited (see [13] for a review). Based on these actuators, several haptic interfaces have been realized with the aim of achieving good dynamic behavior and high transparency, and their MR compatibility has been evaluated. Izawa et al. developed an MR-compatible manipulandum using two ultrasonic motors [10]. Our previous studies have also examined the performance of haptic devices using hydrostatic transmissions [14], ultrasonic motors [11] and electrostatic actuators [15]. As shown in these previous stud-

This work was supported by the Centre d'Imagerie BioMedicale (CIBM) of the University of Lausanne (UNIL), the Swiss Federal Institute of Technology Lausanne (EPFL), the University of Geneva (UniGe), the Centre Hospitalier Universitaire Vaudois (CHUV), the Hopitaux Universitaires de Geneve (HUG) and the Leenaards and the Jeantet Foundations. J. Duenas, D. Chapuis, O. Lambercy and R. Gassert are supported by the NCCR Neural Plasticity and Repair, Swiss National Science Foundation.

M. Hara and H. Bleuler are with the Robotic Systems Lab, EPFL, Lausanne, CH-1024, Switzerland. T. Kober is with the Center for Biomedical Imaging, EPFL, Lausanne, CH-1024, Switzerland.

J. Duenas, D. Chapuis, O. Lambercy, and R. Gassert are with the Rehabilitation Engineering Lab, ETH Zurich, Zurich, CH-8092, Switzerland. Corresponding author's email: gassertr@ethz.ch

ies, the MR compatibility of the aforementioned actuation methods has been demonstrated, but several technical limitations – e.g., limited stroke, non-linearities, low bandwidth, high voltage or high power requirements – have limited their use and haptic performances with respect to conventional robotics technology. This implies that their application fields are narrow and that there is still much room left for further investigation and improvement. It is thus only natural that many groups aim at developing MR-compatible actuation systems with the same ease-of-use and dynamic performance as conventional electromagnetic actuators.

Another approach consists in using conventional electromagnetic actuators and isolating them from the scanner's influence and from disturbing the imaging. We previously evaluated the use of electromagnetic motors in the MR environment [13] to remotely actuate a wrist interface for neuroscience studies to investigate human motor control. However, due to safety and electromagnetic compatibility considerations, especially when large interaction forces are to be generated, the use of conventional actuators in robotic systems for MR applications has so far widely been avoided. Nevertheless, Hribar et al. demonstrated that a PHANToM (SensAble Technology) with a long mechanical extension can be used in an MR environment [16], but no detailed evaluation of MR compatibility was presented. Li et al. [17] also proposed a shielded actuation box to drive a 3-DOF parallel linkage over rods of about 1.8 m length. This box is connected to power and control hardware located in the control room over BNC cable links. Again, only limited compatibility testing was performed.

This paper describes the design of a novel, MRI-compatible high-performance actuation system based on a shielding concept with the aim of achieving the same transparency and dynamic performance as has been achieved with conventional haptics technology. This is a prerequisite for the development of novel robotic systems to investigate the neural control of fine motor control and highly dynamic interactions. We propose an adapted shielding and power/control concept, evaluate the ideal location within the MR environment, and present a detailed evaluation of the MR compatibility of this novel actuation system, taking into account the potential adverse effects of rotating magnetic fields generated by the actuator on the imaging quality of the MR system, as well as the influence of the strong magnetic field and associated spatial gradient on the actuator.

II. Design of a Shielded Actuation System for Applications in MR Environments

We aim to design a novel actuation system that can achieve performance similar to that of conventional electromagnetic actuators to render precise and highly dynamic interactions with human motion during fMRI. Placing a conventional electromagnetic actuator in the control room, outside the shielded MR room, greatly limits the risk of safety hazards and mutual electromagnetic interference. A light yet stiff rod or cable transmission could link the actuator to the slave device located in the MR room. However, this approach suffers from the need of a fixed mechanical structure in the MR room to guide the cables or rods and presents very limited flexibility. These limitations could be overcome by incorporating a penetration panel allowing direct line access from the control room to the slave interface. This is, however, impracticable, and can be overcome by adequately shielding the actuator and electronics, and placing them within the MR environment, in a region in which the local magnetic field strength is low compared to the imaging region (Fig. 1). The actuation system should be placed in a way to avoid acceleration within the spatial gradient of the static magnetic field (safety), and shielded to prevent the actuator from disturbing the imaging, and to avoid performance degradation due to the external electromagnetic fields (electromagnetic compatibility).

A. Shielding Principle

In this work, we attempted to isolate an electromagnetic motor from the electromagnetic fields generated by the scanner and vice versa by using a Faraday cage made of aluminum and a ferromagnetic box made of steel, respectively (Fig. 2). A Faraday cage (or Faraday shield) is a space surrounded by conducting material or by a mesh of such material. In general, the electrical line of force cannot penetrate the space surrounded by the conducting body. Therefore, the static electrical field from outside can be blocked out and all electrical potentials within the conducting body are equalized [18]. Conversely, the effect of an electrical field from the inside to the outside can also be eliminated.

The Faraday cage can also be employed as a magnetic shield, but it is ineffective for static or slowly varying magnetic fields below approximately 100 kHz. fMRI requires a strong static magnetic field of typically 1.5 – 3 T, which rapidly drops off with increasing distance from the magnet. Hence, we also require a magnetic shield. There are only limited possible ways to magnetically insulate a space from an inner or outer magnetic field by surrounding the space with materials of high magnetic permeability such as steel, Permalloy, and Mu-metal. These materials themselves cannot block off the magnetic field, but can create paths for the magnetic field lines around the space, as long as saturation is avoided. The ferromagnetic shield also prevents magnetic fields generated within from being emitted to the outside.

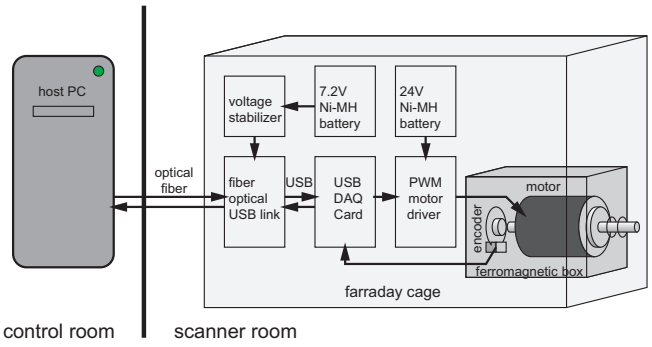

Fig. 2. Schematic layout of the shielded actuation system.

The electromagnetic motor and all peripheral devices are boxed in these shields as shown in Fig. 2. The magnetic shield is used to prevent any dynamically varying magnetic fields generated by the electromagnetic motor during current control operation from disturbing the imaging, as well as to avoid performance degradation due to the local magnetic field during current control of the motor. The Faraday cage prevents any mutual interference in the RF range. We expect that these shields will enable the electromagnetic motor to achieve the same performance as in a normal environment without disturbing the MR imaging.

B. Prototype Actuation System

The components of the prototype shielded actuation system used for MR compatibility evaluation are shown in Fig. 3. All components are enclosed within an aluminum Faraday cage ($450 \times 250 \times 130$ mm), and are standard components used in robotics applications. We use a conventional electromagnetic motor (RE 40, Maxon Motor, Switzerland), a torque limiter, a motor driver (4-Q-DC Servoamplifier ADS 50/5, Maxon Motor), a data acquisition card (NI USB-6221, National Instruments, USA), a USB fiberoptical link with a length of 10 m (USB M2-100/10S, Opticis, Korea) for data communication, a 7.2 V NiMH rechargeable battery back to power the control electronics, and two 12 V NiMH rechargeable battery packs in series to power the motor amplifiers, which are configured in current control mode. In addition, the electromagnetic actuator is surrounded by a small ferromagnetic box ($160 \times 100 \times 50$ mm) made of steel in order to reduce the influence of the magnetic field emitted by the motor and to reduce the local external magnetic field so as to minimize performance degradation due to saturation.

A GUI-enabled application was programmed in Visual C++ (Microsoft, USA), allowing the operator to easily and quickly change the control modes and parameters by a few keystrokes. The operator can also observe all the related data during the MR imaging. The sampling time is set to 9 ms and is limited by the fiberoptical USB link (USB 1.1 protocol). Nevertheless, this sampling rate was sufficient for the detailed evaluation of MR compatibility.

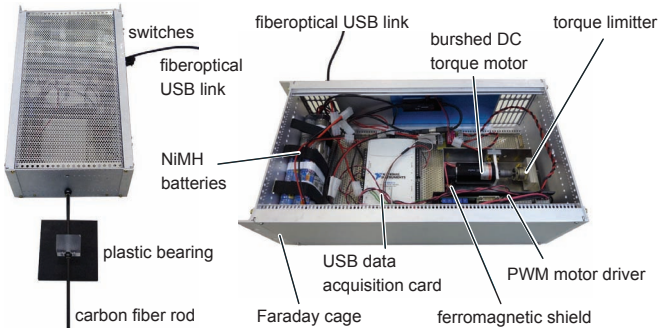

Fig. 3. Pictures of the realized actuation box used for compatibility testing: closed and with extension rod as placed at the end of the scanner bed (left) and open, showing the main system components (right).

C. Validation

To validate this approach, we investigated the intensity of the electromagnetic fields generated by the shielded actuation system by using an electromagnetic field probe (EHP-50C, PMM) and evaluated the efficiency of the selected shielding components. The intensity of the electromagnetic fields emitted by the switching power supply, pulse-width modulation motor controller and DC motor were measured during operation. As expected, the DC motor was found to be the major source of such emission. Fig. 4 shows the intensity of the magnetic field emitted by the unshielded and shielded DC motor when a 50 Hz sinusoidal current with a peak-to-peak amplitude of 10 A was sent through the motor (worst case scenario). In order to reveal the relationship between the intensity of the electromagnetic field and the distance from the measured component, the location of the probe was varied from 0 to 0.4 m in steps of 0.1 m.

The electrical field measurements revealed no significant difference between the two conditions. This is because the ferromagnetic shield can only shield off magnetic fields. In return, the influence of magnetic fields emitted by the electromagnetic motor could be significantly reduced by the use of a ferromagnetic shield, as shown in Fig. 4. Further, since the resolution of the MRI scanner used for our test is about 0.3 μT (magnetic field stability of about 0.1 ppm), Fig. 4 shows that the ferromagnetic shield would enable placing the motor just 0.2 m away from the scanner. Without the ferromagnetic shield, the motor should be placed at least 0.3 m away from the scanner. In reality, the motor will be placed even further away to avoid saturation of the magnetic shield due to the external magnetic field generated by the scanner, and also to ensure safety. However, the effective MR compatibility of this setup can only be confirmed through an in-depth analysis in the real environment, which we present in section III-C.

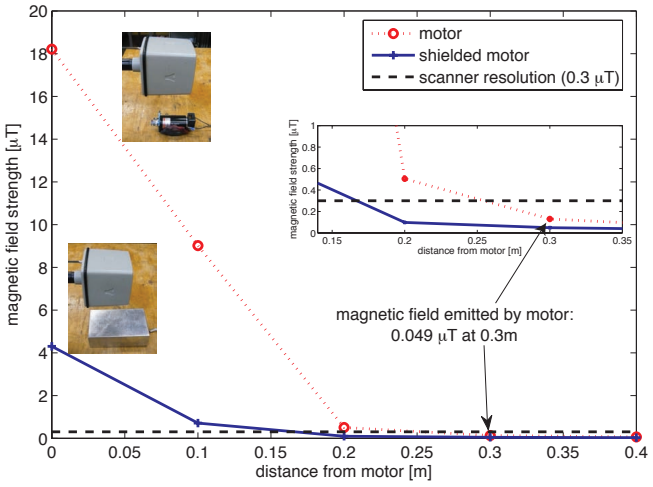

Fig. 4. Magnetic field emitted by the unshielded (dotted line) and shielded (continuous line) DC motor, measured by an electromagnetic field probe (gray block). The dashed horizontal line shows the resolution of the scanner, which is already undercut at a distance of 0.3 m (inlet).

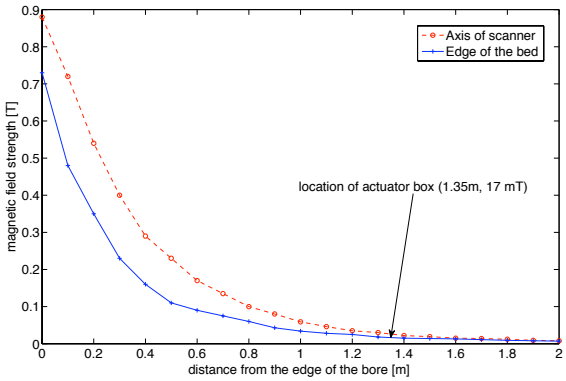

Fig. 5. Spatial magnetic field gradient of a Siemens Tim Trio 3 T scanner along the axis of the magnet and the edge of the scanner bed.

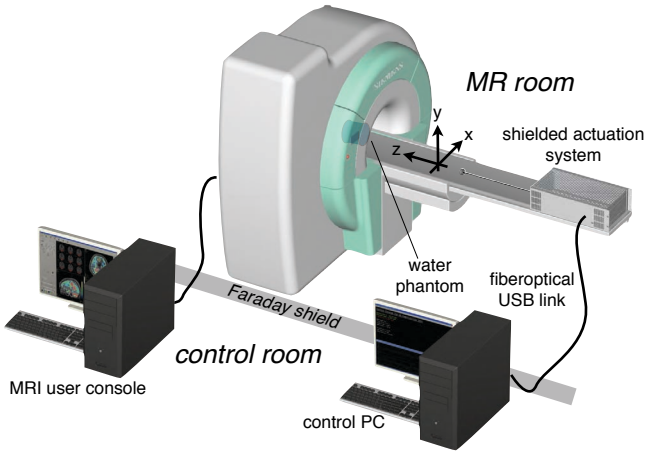

Fig. 6. Experimental setup within the MR environment. A fiber-optical USB cable links the power and control hardware located within the Faraday cage to a PC in the control room.

III. Evaluation in an MR Environment

As a next step the shielded actuation system was installed in an MR environment to evaluate system performance and MR compatibility (Fig. 6).

A. Safety and Placement

Safety and compatibility tests were performed in a 3 T scanner (Siemens Tim Trio, Erlangen, Germany) at the Centre Hospitalier Universitaire Vaudois (CHUV) in Lausanne. In order to determine the optimal placement of the actuation system, we measured the intensity of the magnetic field in function of the difference from the edge of the scanner bore using a commercial teslameter (Digital Teslameter FM 210, Project Elektronik, Berlin, Germany) (Fig. 5). Fig. 6 shows the experimental setup as installed within the MR room during compatibility tests and performance evaluation. As the designed actuation system contains several magnetic components, safety is crucial and must be ensured during practical use. This was achieved by replacing all the ferromagnetic screws of the rack with brass screws, and securing the Faraday cage against the door of the scanner room over a Kevlar cable (safety precaution), as shown in Fig. 1. The actuation system is located at the end of the retracted scanner bed, about 1.35 m away from the edge of the scanner bore. This distance was selected based on safety considerations and to protect the control electronics. The local magnetic field strength was determined to be about 17 mT (Fig. 5). This assures that the gravitational force on the actuation system is higher than the attractive force generated by the spatial gradient of the static magnetic field, thereby preventing acceleration into the scanner bore, and places the system outside the critical 20 mT line, which delimits the region into which conventional and sensitive equipment can be brought with adequate precautions. Torque and motion of the motor can then be transmitted to the haptic display over a rod/cable transmission, or over a timing belt. In a previous study, good dynamic behavior was demonstrated using such an actuation system to control a slave interface located up to 2 m away, at the entry of the scanner bore, over a cable transmission [19]. Even with this distance, an open-loop force control bandwidth of 16 Hz was achieved, which is sufficient for human machine interaction.

B. Actuator Performance

Several control modes – current, velocity, and position profiles – were implemented to drive the shielded electromagnetic motor in the MR environment in order to verify the MR compatibility and to compare control performance in the lab and MR environment. Here we focus on current control, which generates dynamic variations in the magnetic field and is the typical control mode in haptics applications. In the experiment, a 0.25 Hz square current signal of ± 5.0 A (the maximum continuous current the motor driver can output) was applied to the motor. A torque limiter was employed to generate load on the motor shaft and thereby simulate interaction with a user. The motor current was measured at the current monitor output of the employed motor driver. Fig. 7 compares motor performance in current control mode in the lab and MR environment. No significant difference was found between the two conditions (correlation coefficient of 0.998). Similarly, no degradation of motor performance was found in velocity and position control mode. This implies that the Faraday cage and ferromagnetic shield are effective in blocking off the electromagnetic fields of the scanner.

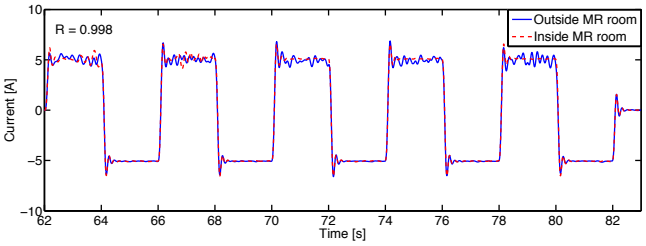

Fig. 7. Current control performance of the electromagnetic motor in the lab and MR environment.

C. MR Compatibility Tests

1) Measurements: All measurements were performed on a Siemens Tim Trio 3 T scanner using a 12-channel head coil (Siemens) and a 7.3 l cylindrical water phantom (1.25 g $NiSO_4 \times 6\ H_2O$ / 2.62 g $NaCl$ per 1000 g H_2O) as coil loading. Field maps (36 slices, slice thickness 3 mm+25% distance factor, FoV 192×192 mm^2, TR 488 ms, TE1/TE2 4.92/7.38 ms) were acquired before and after installing the actuation system in the scanner room, as well as after powering it. No shim adjustment was performed between these scans. Therewith, any static change of the magnetic field due to the metal close to the scanner could be investigated. In order to test for any interferences with the image acquisition, an EPI sequence (34 slices, TR 2 s, TE 30 ms, FoV 192×212 mm^2, matrix 58×64, voxel size $3.3 \times 3.3 \times 3.3$ mm^3) which was extended by a free induction decay (FID) navigator module [20] was employed. This navigator sampled 128 points in the center of the k-space before each slice readout train. Its high sensitivity to field changes, which are reported being able to detect respiratory-induced field fluctuations, suggested it as a mean to detect dynamic field changes caused by the actuator. With the given repetition time and number of slices, the sampling frequency of the phase navigator was 17 Hz. Finally, a gradient echo sequence (1 slice), whose excitation pulses were switched off, was used to test for RF interference caused by the actuation system. The resulting noise image allowed for detection of any RF signal within the bandwidth used by the imaging procedure.

2) Data Analysis: The phase of the averaged 128 k-space center sample points was calculated, yielding one phase data point per slice. Navigator phase offsets between the slices were eliminated by normalizing each phase data point with the data point in the corresponding slice of the first repetition. In the course of an MR experiment, the main magnetic field B0 fluctuates minimally due to system-related effects (i.e. heating). To compensate for this effect, zero and first order drifts were subtracted from the navigator signal course by means of a linear regression. Differences in the B0-field before/after installing the actuation system, as well as in silent/powered mode were calculated by subtracting the corresponding field maps. In order to investigate the spatial variation of the differences in all three spatial directions, a ROI of 3×3 voxels was averaged in the middle of each image plane, yielding one field difference value per plane. A linear regression was performed on these data points going through the image planes in x-, y- and z-direction. Data points from empty slices (i.e. containing no signal from the phantom) were ignored.

3) Results: The phase navigator showed negligible changes in the frequency distribution of the phase navigator signal. The field maps (Fig. 8) showed no difference in x- and y-direction as expected. However, a very small change between 0.12 Hz/m and 0.31 Hz/m could be detected along the z-direction, which can also be considered negligible, and can easily be compensated by shimming. For comparison, in a typical fMRI measurement there is a difference of 20 Hz between the voxels in the phase encoding direction. The coefficient of variation of the RF interference noise images was not changed by any of the tested cases, i.e. no RF interference was observed.

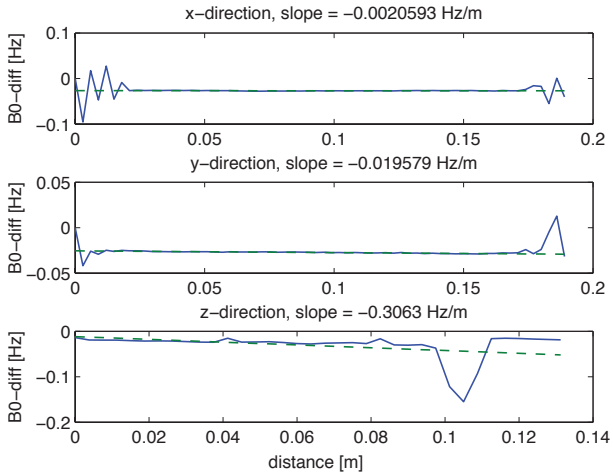

Fig. 8. Comparison of magnetic field maps acquired without the shielded actuator (dashed) and with the powered actuator placed at the extremity of the retracted scanner bed (continuous line). The variations at either extremity result from background noise (measurements outside the phantom).

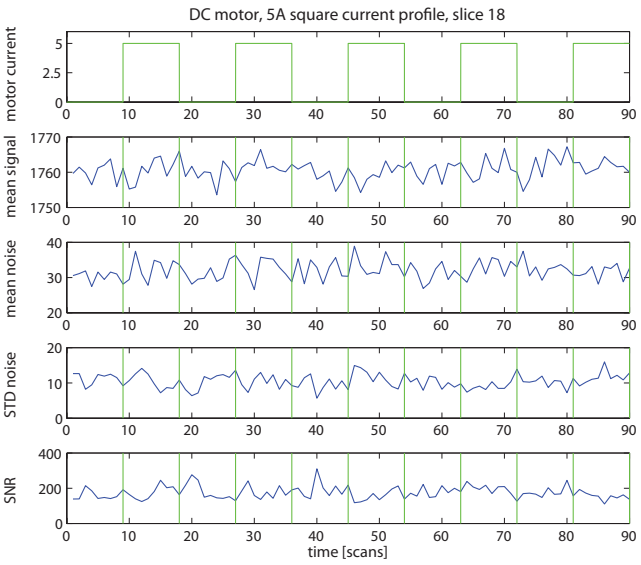

Fig. 9. Mean signal, mean noise, standard deviation of noise and signal-to-noise ratio of slice 18 over 5 repetitions of silent (0 A) and powered (5 A) actuator conditions. A t-test revealed no significant differences between the SNR variation in the two conditions.

Further, we compared the variance of the signal-to-noise ratio (SNR) between the silent and powered conditions, in which the motor was driven with a 5 A square current signal (Fig. 9). A two-sampled t-test revealed no significant difference between the two conditions (p=0.33).

Finally, we also performed an image subtraction between slice number 18 (located in the center of the phantom) of scan 14 (powered condition) and scan 5 (silent condition), which revealed no image shifts or deformations. We thereby

conclude that there is no detectable influence of the actuation system on the imaging.

IV. Conclusions

We have proposed a novel shielded actuation concept allowing the use of a conventional electromagnetic actuator within an MR environment while guaranteeing safety and mutual electromagnetic compatibility. This approach brings the good dynamic behavior of conventional direct-drive electromagnetic actuators to MR-compatible robotics applications, opening new avenues for fMRI-based neuroscience studies investigating the neural correlates of fine motor control of the hand and fingers as well as related dysfunctions. The electromagnetic actuator is located within a shielded steel box to prevent disturbance from the dynamically changing magnetic fields of the motor on the scanner, as well as to prevent any performance degradation of the motor from the local magnetic field generated by the scanner. Power and control hardware are contained within a Faraday cage with only a fiber-optical USB link to the control room, in order to prevent electromagnetic interference. Detailed compatibility tests beyond what has previously been presented in the literature were carried out to investigate the influence of static and dynamic variations of the magnetic field as well as RF interference created from the operation of the actuation system on the imaging. These tests revealed undetectable or negligible influence on the imaging, showing the effectiveness of the proposed shielding concept. Furthermore, actuator performance was found not to be degraded by the scanner with respect to operation in a lab environment. To assure safety and protect control electronics, the presented actuation system is ideally placed at the far end of the scanner bed, about 1.35 m away from the edge of the scanner bore. Motion and force can be transmitted over a light and rigid cable or rod transmission, thereby guaranteeing good transparency and high force control bandwidth. In a recent proof-of-principle study, we demonstrated the good dynamic performance of such a transmission, achieving a 16 Hz open-loop force bandwidth [19]. This novel actuation method is ideal to drive image-guided interventional robots for minimally invasive surgery, and haptic interfaces for dynamic interaction with human motion in functional neuroscience studies.

V. Acknowledgements

We thank Jordi Campos Carol and Francois Barrot for their contribution to the design and evaluation of the shielded actuator, as well as Gunnar Krueger and the staff of the imaging center at the University Hospital Vaudois (CHUV) for the valuable discussions and support during the compatibility tests.

References

[1] A. Bardorfer, M. Munih, A. Zupan, and A. Primozic, "Upper limb motion analysis using haptic interface," *IEEE/ASME transactions on Mechatronics*, vol. 6, no. 3, pp. 253–260, 2001.

[2] D. Heeger and D. Ress, "What does fMRI tell us about neuronal activity?" *Nature Rev Neurosci*, vol. 3, no. 2, pp. 142–151, 2002.

[3] G. Buccino, F. Binkofski, G. Fink, L. Fadiga, L. Fogassi, V. Gallese, R. Seitz, K. Zilles, G. Rizzolatti, and H. Freund, "Action observation activates premotor and parietal areas in a somatotopic manner: an fMRI study." *European Journal of Neuroscience*, vol. 13, no. 2, p. 400, 2001.

[4] N. S. Ward, J. M. Newton, O. B. C. Swayne, L. Lee, A. J. Thompson, R. J. Greenwood, J. C. Rothwell, and R. S. J. Frackowiak, "Motor system activation after subcortical stroke depends on corticospinal system integrity." *Brain*, vol. 129, no. Pt 3, pp. 809–819, 2006.

[5] B. Schueler, T. Parrish, J. Lin, B. Hammer, B. Pangrle, E. Ritenour, J. Kucharczyk, and C. Truwit, "MRI compatibility and visibility assessment of implantable medical devices," *Journal of Magnetic Resonance Imaging*, vol. 9, no. 4, pp. 596–603, 1999.

[6] R. Gassert, E. Burdet, and K. Chinzei, "Opportunities and Challenges in MR-Compatible Robotics," *IEEE Engineering in Medicine and Biology Magazine*, vol. 27, no. 3, pp. 15–22, 2008.

[7] K. Uffmann, C. Abicht, W. Grote, H. Quick, and M. Ladd, "Design of an MR-compatible piezoelectric actuator for MR elastography," *Concepts in Magnetic Resonance*, vol. 15, no. 4, 2002.

[8] R. Gassert, L. Dovat, O. Lambercy, Y. Ruffieux, D. Chapuis, G. Ganesh, E. Burdet, and H. Bleuler, "A 2-DOF fMRI compatible haptic interface to investigate the neural control of arm movements," in *IEEE International Conference on Robotics and Automation (ICRA)*, 2006, pp. 3825–3831.

[9] N. Yu, W. Murr, A. Blickenstorfer, S. Kollias, and R. Riener, "An fMRI compatible haptic interface with pneumatic actuation," *Proc. IEEE 10th International Conference on Rehabilitation Robotics (ICORR)*, 2007.

[10] J. Izawa, T. Shimizu, H. Gomi, S. Toyama, and K. Ito, "MR compatible manipulandum with ultrasonic motor for fMRI studies," in *Proceedings 2006 IEEE International Conference on Robotics and Automation*, 2006, pp. 3850–3854.

[11] D. Chapuis, R. Gassert, E. Burdet, and H. Bleuler, "A hybrid ultrasonic motor and electrorheological fluid clutch actuator for force-feedback in MRI/fMRI," in *IEEE Engineering in Medicine and Biology Society Conference (EMBC)*, 2008, pp. 3438–42.

[12] A. Yamamoto, K. Ichiyanagi, T. Higuchi, H. Imamizu, R. Gassert, M. Ingold, L. Sache, and H. Bleuler, "Evaluation of MR-compatibility of electrostatic linear motor," in *Proc. IEEE International Conference on Robotics and Automation (ICRA)*, 2005, pp. 3658–3663.

[13] R. Gassert, A. Yamamoto, D. Chapuis, L. Dovat, H. Bleuler, and E. Burdet, "Actuation methods for applications in MR environments," *Concepts in Magnetic Resonance Part B: Magnetic Resonance Engineering*, no. 4, pp. 191—209, 2006.

[14] R. Gassert, R. Moser, E. Burdet, and H. Bleuler, "MRI/fMRI-compatible robotic system with force feedback for interaction with human motion," *IEEE/ASME Transactions on Mechatronics*, vol. 11, no. 2, pp. 216–224, 2006.

[15] M. Hara, G. Matthey, A. Yamamoto, D. Chapuis, R. Gassert, H. Bleuler, and T. Higuchi, "Development of a 2-DOF electrostatic haptic joystick for MRI/fMRI applications," in *IEEE International Conference on Robotics and Automation (ICRA)*, 2009, pp. 1479–1484.

[16] A. Hribar, B. Koritnik, and M. Munih, "Phantom haptic device upgrade for use in fMRI," *Medical and Biological Engineering and Computing*, vol. 47, no. 6, pp. 677–684, 2009.

[17] S. Li, A. Frisoli, L. Borelli, M. Bergamasco, M. Raabe, and M. W. Greenlee, "Design of a new fMRI compatible haptic interface," in *WHC '09: Proceedings of the World Haptics 2009 - Third Joint EuroHaptics conference and Symposium on Haptic Interfaces for Virtual Environment and Teleoperator Systems*. Washington, DC, USA: IEEE Computer Society, 2009, pp. 535–540.

[18] R. Elliott, *Electromagnetics: history, theory, and applications*. Wiley-IEEE Press, 1999.

[19] J. Duenas, O. Lambercy, D. Chapuis, and R. Gassert, "ReGrasp, a robotic tool to investigate fine motor control and track therapy-induced neuroplasticity." *IEEE International Conference on Robotics and Automation (ICRA)*, pp. 5084–5089, 2010.

[20] J. Pfeuffer, P.-F. Van de Moortele, K. Ugurbil, X. Hu, and G. H. Glover, "Correction of physiologically induced global off-resonance effects in dynamic echo-planar and spiral functional imaging," *Magn Reson Med*, vol. 47, no. 2, pp. 344–53, Feb 2002.